Development of Porous Alginate Microbeads Containing Silver Nanoparticles and Their Antibacterial Efficacy

M. R. EL-AASSAR

College of Chemistry, Chemical Engineering and Biotechnology, Donghua University, Shanghai 201620, People's Republic of China

Polymer Materials Research Department, Advanced Technology and New Material Research Institute, City of Scientific Research and Technological Applications (SRTA-City), New Borg El-Arab City 21934, Alexandria, Egypt

XIUMEI MO

College of Chemistry, Chemical Engineering and Biotechnology, Donghua University, Shanghai 201620, People's Republic of China

Correspondence to: M. R. El-Aassar; e-mail: mohamed_elaassar@yahoo.com; Xiumei Mo; e-mail: xmm@dhu.edu.cn

Received: April 27, 2015
Accepted: June 30, 2015

ABSTRACT: The main aim of this study is to develop a new method to prepare porous microbeads. Silver nanoparticles (AgNPs) were synthesized in an alginate colloidal solution, and then the porous microbeads containing AgNPs were prepared. The prepared alginate/AgNPs microbeads were ~300 μm in diameter. The resulting alginate/AgNPs microbeads were placed in a solvent of *N*,*N*-dimethylformamide with AgNPs, which resulted in the formation of pores in the block microbeads composite. The formation of AgNPs was confirmed by UV–vis spectroscopy and TEM; the results showed that the AgNPs have a diameter range of 6–21 nm. The microbeads are characterized by using SEM, EDX, as well as FTIR. The porous alginate/AgNPs microbeads were examined against different pathogenic bacterial strains, and the result was compared with another alginate/AgNPs microbeads. The porous alginate/AgNPs microbeads exhibit a strong antimicrobial activity compared to the alginate/AgNPs microbeads. Adv Polym Technol 2016, 35, 21555; View this article online at wileyonlinelibrary.com. DOI 10.1002/adv.21555

KEY WORDS: Biopolymers, Diffusion, Nanoparticles, Nanostructure, Antibacterial

Introduction

Alginate is a linear polysaccharide derived from the marine brown algae or produced by bacteria, naturally occurring copolymer composed of α- poly-β-1, 4-D-mannuronic acid (M) and α -1, 4-L-glucuronic acid (G). Alginate has some unique properties such as water solubility, biocompatibility, nonantigenicity, renewability, and biodegradability in tissue, and it is considered to be a nontoxic substance.[1] Alginate has attracted considerable attention for its wide range of uses in the industrial and medical applications.[2] Moreover, alginate can form strong gels by metal cation interaction such as calcium (Ca^{2+}) ions.[3] Also, sodium alginate hydrogel is commercially used in various medical applications, such as drug delivery,[4–6] cell,[7] enzyme,[8] and tissue engineering and wound dressings.[9,10] In addition, the sodium alginate has attracted significant interest as biopolymers because of their unique properties such as ecofriendliness and compatibility and increasing use in biomedical applications and pharmaceutical. The pore structure is the important factor that affects the characteristics of the materials. All these factors are closely related to the porous structures such as surface area, pore size, permeability, and pore volume. So, the control and distributions of pore structures is a highly desirable attribute.[11] Also, the diffusion and interaction of the nanoparticles are also required, because the size distribution of nanoporous in microbeads and the biological interaction of nanoparticles with the biological cells are generally affected by the porous size and of the particles.[12] Many different methods have been proposed to prepare microspheres with porous structures. The antibacterial materials are commonly used to effectively protect the human health in everyday life. Bacterial contamination of body substances and environmental, especially with medical equipment, has attracted much attention since the discovery of antibacterial materials. Therefore, the development of resistance against them is highly desirable. A wide variety of materials and technologies that provide antimicrobial agents, including metal ions, antibiotics, and silver nanoparticles (AgNPs), are also interesting materials for wound-dressing applications.[13] However, these materials are known to be associated with environmental pollution, antibiotic resistance, high cost, and complex processing. In recent times, antibacterial properties of nanomaterials offer effective solutions against these challenges, including AgNPs[14] and metal oxide nanoparticles.[15] AgNPs have been a major focus for their use as antimicrobial agents, catalysts, and optical sensors.[16–23] AgNPs as antibacterial agents have increasingly

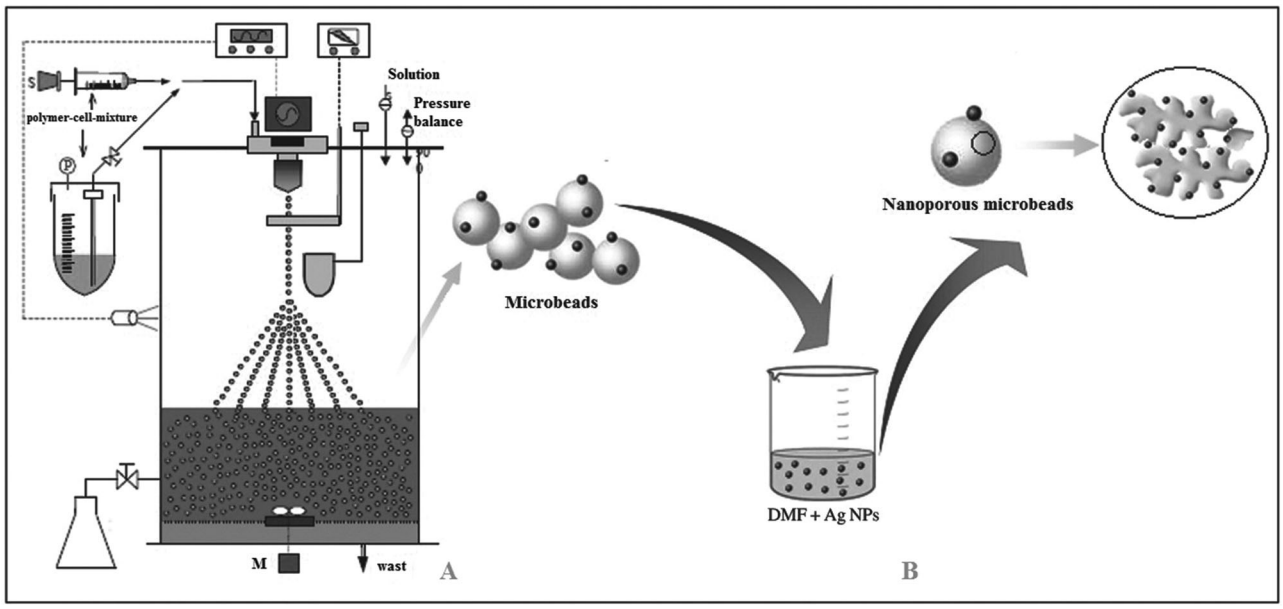

FIGURE 1. Schematic diagram represents the formation of porous alginate/AgNPs microbeads using encapsulator.

been used in medical applications due to their good compatibility with other materials, chemical inertness, and higher surface area to volume ratio, comparable to the bulk form.[24] However, AgNPs with small particle sizes and Particle size distribution of the AgNPs, a crucial issue about AgNPs is their tendency to aggregate due to their high surface energy. One strategy of preventing aggregation of the silver particles is the controlled deposition of metal particles through hybridization by using a nanoporous material as the matrix to ensure the distribution of the AgNPs.[25,26] The reported examples of templates included polymers[27,28], surfactants.[29]

In this work, AgNPs were synthesized using alkali hydrolyzed sodium alginate. The resulting alginate/AgNPs microbeads are placed in a solvent of DMF with AgNPs for fabrication of the porous structure in the alginate/AgNPs microbeads. The characteristics of alginate/AgNPs porous structure were examined by scanning electron microscopy (SEM), energy dispersive X-ray spectroscopy (EDX), and Fourier transform infrared spectroscopy (FTIR). Finally, the antimicrobial performances were determined by using *Staphylococcus aureus*, *Micrococcus luteus*, *Escherichia coli*, and *Pseudomonas aeruginosa* as the model bacteria.

Materials and Methods

MATERIALS

Sodium alginate with a viscosity of 15,000–20,000 centipoises, silver nitrate ($AgNO_3$) (99.9%), calcium chloride anhydrous, and *N*,*N*-dimethyl formamide (DMF) were obtained from Sigma-Aldrich (Schnelldorf, Germany). Distilled water was used throughout this research. All other chemicals were of analytical grade and were used without any further purification.

PREPARATION OF ALGINATE/AGNPS SUSPENSION

Sodium alginate solution (1.5 %) was prepared by dissolving in 100 mL of hot distilled water using a magnetic stirrer until complete homogenization was achieved. Hydrolysis of sodium alginate solution by sodium hydroxide (NaOH) aqueous solution with continuous stirring for 10 min for the preparation of alkaline sodium alginate solution with pH = 12.0. After that, the temperature of the reaction medium was gradually raised to 60–80ºC. The silver nitrate ($AgNO_3$) solution (0.3 mol/L) was gradually added to the alginate solution with magnetic stirring.[30] The change in color of the solution from colorless to the yellow and from yellowish color to brownish color, indicated formation of AgNPs suspension.

ALGINATE/AgNPs MICROBEADS PREPARATION

For the preparation of alginate/AgNPs microbeads, the alginate/AgNPs suspension was dropped through a spray nozzle of 300 μm using an Inotech encapsulator IER-50 (Switzerland) with voltage in the range of 400—1700 V (Fig. 1A).[2] The syringe was used to pump the alginate/AgNPs suspension and was connected to a spray nozzle by a plastic tube. This operation was adjusted at a frequency of 550 Hz, a voltage was set to 1400 V, and the infusion rate was 10 mL/h. The resulting microbeads were dripped into a cross-linking solution containing 3% $CaCl_2$ solution for solidification with continuously stirring for 30 min. The AgNPs embedded in the alginate microbeads were collected from the cross-linking solution using a sieve. Finally, the alginate/AgNPs microbeads were rinsed twice with

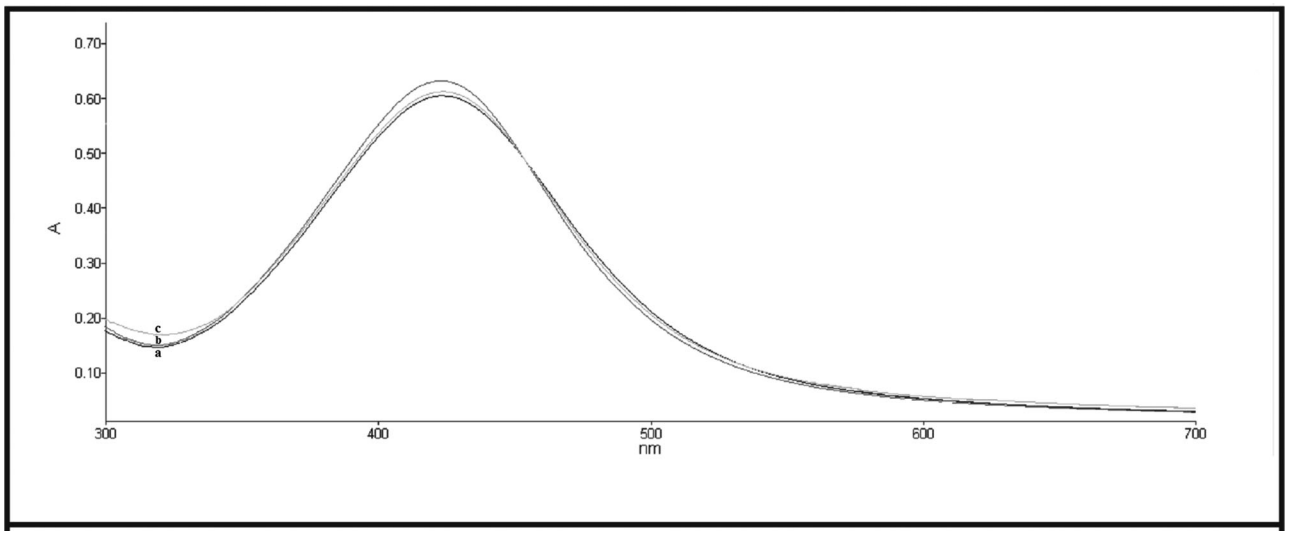

FIGURE 2. UV–vis spectroscopy of AgNPs solutions for (a) 0.1 mol/L $AgNO_3$ colloidal solutions, (b) 0.3 mol/L $AgNO_3$ colloidal solutions, and (c) DMF/AgNPs solutions.

water and the surface excessive water on the microbeads was wiped by tissue paper.

PREPARATION POROUS STRUCTURE OF ALGINATE/AgNPs MICROBEADS

$AgNO_3$ (0.03 mol/L) was dissolved in DMF into the beaker under mild magnetic stirring, and the original color of DMF changed to the yellow color with the formation of AgNPs in DMF solution.[31] Subsequently, approximately 1 g of alginate/AgNPs microbeads was transferred to DMF/AgNPs solution under continuous stirring for 30 min to prepare the porous alginate/AgNPs microbeads (Fig. 1B). The obtained porous alginate/AgNPs microbeads were collected by using a sieve, and the microbeads were washed many times with distilled water. Thus the porous alginate/AgNPs were obtained.

CHARACTERIZATION OF AgNPs AND POROUS ALGINATE/AgNPs MICROBEADS

UV–Vis Spectroscopy

The presence of AgNPs in alginate colloidal solutions and DMF solution was determined using UV–vis spectroscopy (Ultrospec 2000; UK), in the wavelength range between 300 and 700 nm, the distilled water and DMF solvent used as a blank reference.

Transmission Electron Microscopy

The particle size and morphology of AgNPs were analyzed by the transmission electron microscope (JEOL JEM 2100) operating at a voltage of 200 kV. The images obtained through the transmission electron microscope were used to analyze AgNPs' particle size.

Particles Size Analysis

The particles size and particles size distribution of AgNPs was monitored by using a submicron particle size analyzer (Beckman Coulter). The AgNPs in alginate colloidal solution were dispersed in water, at a temperature of 20 ºC, viscosity 1.0, and refractive index 1.33.

Scanning Electron Microscopy and Energy Dispersive X-Ray Spectroscopy

Morphological characteristics of alginate and porous alginate/AgNPs microbeads were analyzed by a scanning electron microscope (JEOL, JSM-6360LA; Japan) at a smaller magnification. Alginate and porous alginate/AgNPs microbeads were fixed onto the specimen holder and was covered by gold-coated layers by the sputtering method. The SEM images were taken at a magnification of 500×, 5000×, and 10,000× using 10 kV accelerating voltage. The chemical and elemental characterizations of porous alginate/AgNPs microbeads were obtained using an energy dispersive X-Ray spectroscope (JEOL, JSM-6360LA; Japan).

X-Ray Diffraction and Fourier Transform Infrared Spectroscopy

The structure of porous alginate/AgNPs microbeads were studied by X-ray diffraction (XRD; Shimadzu XRD 7000, Japan), and FTIR (Shimadzu FT-IR8400 S, Japan), in the spectral range of 4000–400 cm^{-1} in the absorbance mode.

EVALUATION OF ANTIMICROBIAL ACTIVITY

The antimicrobial effects of alginate, alginate/AgNPs, and porous alginate/AgNPs microbeads were tested against Gram-positive and Gram-negative bacterial strains by the zone of inhibition test. The diameter of the inhibition zone was recorded

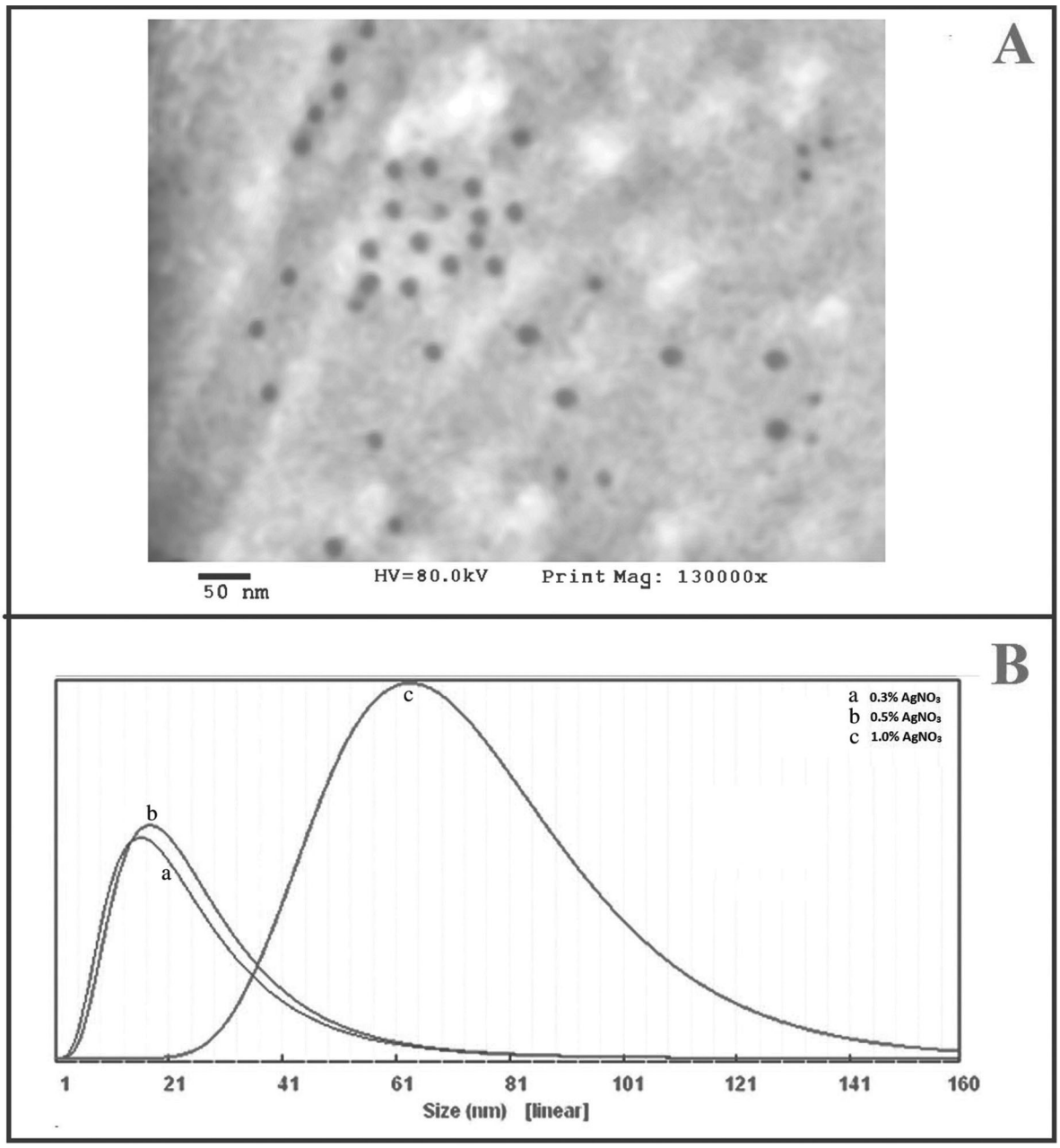

FIGURE 3. TEM images and particle size distribution graph of AgNPs formed alginate colloidal solutions: (A) TEM micrograph of AgNPs and (B) size distribution and size average for AgNPs in the viewed TEM image.

against the Gram-positive bacteria, *S. aureus* (ATCC 25923) and *M. luteus* (ATCC 15307), and the Gram-negative bacteria, *E. coli* (ATCC 25922) and *P. aeruginosa* (ATCC 27853). Briefly, the bacterial colonies from each strain were suspended in 5 mL of Mueller—Hinton solution until the visible turbidity was equal to the 0.5 MacFarland standards. The suspension of bacterial cultures was made and streaked over the exterior of the agar surface to have uniform microbial growth on the agar. After the agar surfaces were allowed to dry, microbeads were added to the top of the agar. Finally, after 24 h incubation at 35°C, diameters of the zones of growth inhibition were measured. All tests were done in duplicate.

Results and Discussion

CHARACTERIZATION OF THE SYNTHESIZED SILVER NANOPARTICLES

AgNPs were synthesized in water-soluble biopolymers using the alkaline aqueous solution of sodium alginate by heating a mixture of sodium alginate and $AgNO_3$ at 60–80 ºC. Sodium alginate is a natural anionic molecule, has high charge density, contains carboxylic groups, and can provide stable negatively charged AgNPs colloid and exceptional stability against

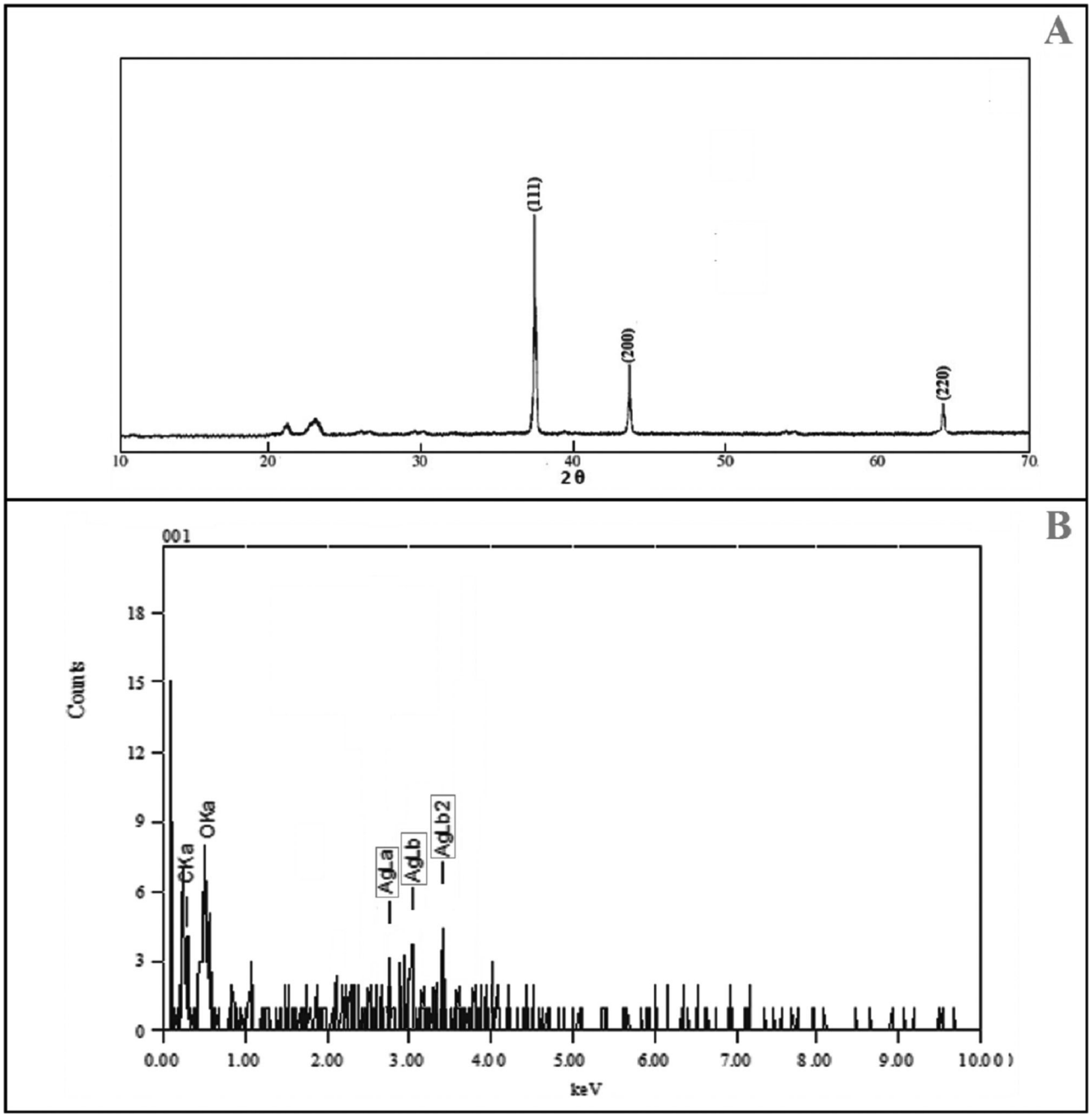

FIGURE 4. (A) XRD patterns of porous alginate/AgNPs microbeads and (B) EDX image for porous alginate/AgNPs microbeads.

agglomeration. Alkali hydrolysis of alginate improves water solubility of alginate and provides higher reducibility for $AgNO_3$.[30] Alkali hydrolysis of sodium alginate acts as a reduction agent and stabilizing agent in the synthesis of AgNPs. The reaction and formation of AgNPs can be easily monitored by the change in color of the solutions. Figure 2 shows the UV–vis absorption spectra of AgNPs colloidal, a solution stabilized by sodium alginate with the $AgNO_3$ concentration of 0.1 (mol/L) (Fig. 2a), 0.3 (mole/L) (Fig. 2b), and AgNPs prepared in DMF (Fig. 2c), The data shown in Figs. 2a–2c suggest that the absorption bands are centered around 412 nm. The maximum absorption band at 412 nm becomes stronger for 0.1 (mol/L) (Fig. 2a), 0.3 (mol/L) (Fig. 2b), and DMF/AgNPs (Fig. 2c), which indicates that the formation of smaller AgNPs and the AgNPs have a sharp size distribution with high dispersion in the solution.[25,32]

The particle size and morphology of the AgNPs formed on the alkaline aqueous solution mixture of sodium alginate and $AgNO_3$ were examined using the transmission electron microscope (Fig. 3A), and this analysis revealed that the AgNPs show spherical morphology, small particle size in the range of 20 nm, and well dispersion in the solution without aggregation. Figure 3B show the average particle size and particle size distribution for AgNPs prepared with different concentrations of $AgNO_3$ (0.1, 0.3, 0.5 mol/L) with alkali hydrolyzed alginate. It is clearly

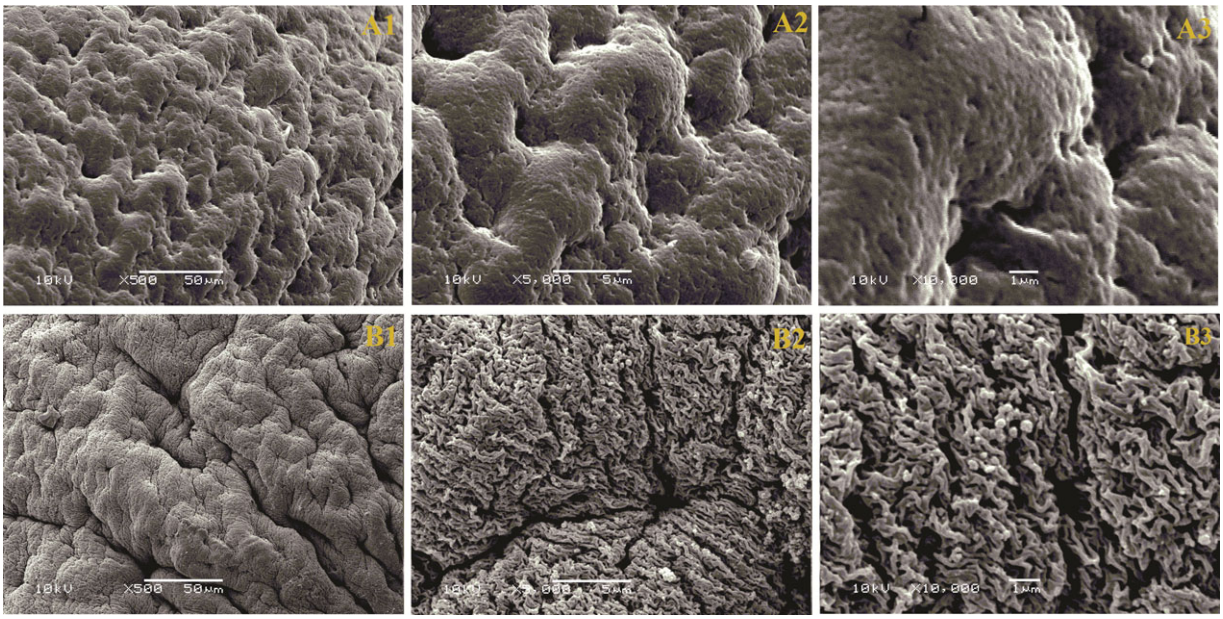

FIGURE 5. SEM image showing surface morphologies of microbeads made from alginate, and porous alginate/AgNPs microbeads at 500× (A1, B1), 5000× (A2, B2), and 10,000× (A3, B3) magnification.

illustrated that the small particles size was detected for both 0.1 and 0.3 mol/L $AgNO_3$ with a 1–70 nm with mainly average size of 6–21 nm; the particles size of the AgNPs increased with the increase in the $AgNO_3$ concentration until the concentration of $AgNO_3$ reaches to 0.5 mol/L. By increasing the concentration of $AgNO_3$ up to 0.5 mol/L, the particles size is increased, which may suggest that the nanoparticles in the solution may be aggregated.

In addition, the crystal structures of prepared spherical Ag nanoparticles can be confirmed by XRD analysis. Figure 4A shows XRD patterns of the porous alginate/AgNPs microbeads, which had well-defined characteristic diffraction peaks at 38.0º, 43.6º, and 64.3º and correspond to diffraction peaks (111), (200), and (220) of the silver crystal, respectively. The sharp peaks indicate the formation of AgNPs with small particle sizes.[34] Figure 4B shows the EDX spectrum of porous alginate/AgNPs microbeads, confirming the existence of Ag element on the surface of the porous alginate/AgNPs microbeads, and EDX images provided evidence for the presence of elemental silver. The EDX results show that carbon, oxygen, and Ag bonds were the principal elements of porous alginate/AgNPs microbeads. Also, the EDX analysis confirms the existence of the AgNPs in the microbeads as a peak of Ag was observed.

MORPHOLOGY OF THE ALGINATE AND POROUS ALGINATE /AgNPs MICROBEADS

The scanning electron micrographs were used to observe the micromorphology and nanoporous network structure of the microbeads. The SEM photographs of the surface morphology of alginate are shown in Figs. 5A1–5 A3, and porous alginate/AgNPs microbeads are shown in Fig. 5B1–5 B3. The SEM images of both sample was compared based on their network structure at different magnification as shown in Fig. 5 (500× (A1 and B1), 5000× (A2 and B2), and 10,000× (A3 and B3)). As shown in Fig. 5, it is clear that the surface structure and morphological characterization of alginate microbeads differ from porous alginate/AgNPs microbeads. Figure 5A3 shows that the surface of alginate microbeads is nonporous and has a smooth surface, but Fig. 5B3 shows high porous structures for the porous alginate/AgNPs microbeads. The difference in the porous structure when using DMF containing AgNPs was confirmed by the pore size measurements; the diameter of the pore size of the porous alginate/AgNPs was determined using software attached to the SEM instrument (Fig. 6A). The results show that the bar diameter of the microbead network varies from 45 to 270 nm (Fig. 6B), whereas the pore size of the structure seems to in the range of 50–300 nm (Fig. 6A); and alginate/AgNPs microbeads with nanoporous structures were successfully prepared.

FTIR ANALYSIS OF THE ALGINATE AND POROUS ALGINATE /AGNPS MICROBEADS

Figure 7 shows FTIR spectra of prepared sodium alginate and porous alginate/AgNPs microbeads. The FTIR absorption spectra of the alginate microbeads and porous alginate/AgNPs microbeads show characteristic OH (stretching vibration bands) at 3439 cm^{-1}. Other observable peaks were detected around 2945 cm^{-1} (CH, aliphatic, stretching), and the C=C stretching vibration of unsaturated aliphatic structures appears at 1625 cm^{-1}. From the above FTIR spectra, the alginate/AgNPs microbeads treated with DMF/AgNPs do not show any change in the molecular structure, and there is no chemical interaction between alginate/AgNPs and DMF/AgNPs; whereas the interaction between microbeads and DMF/AgNPs only changed the surface structure of treated microbeads (Fig. 5B3).

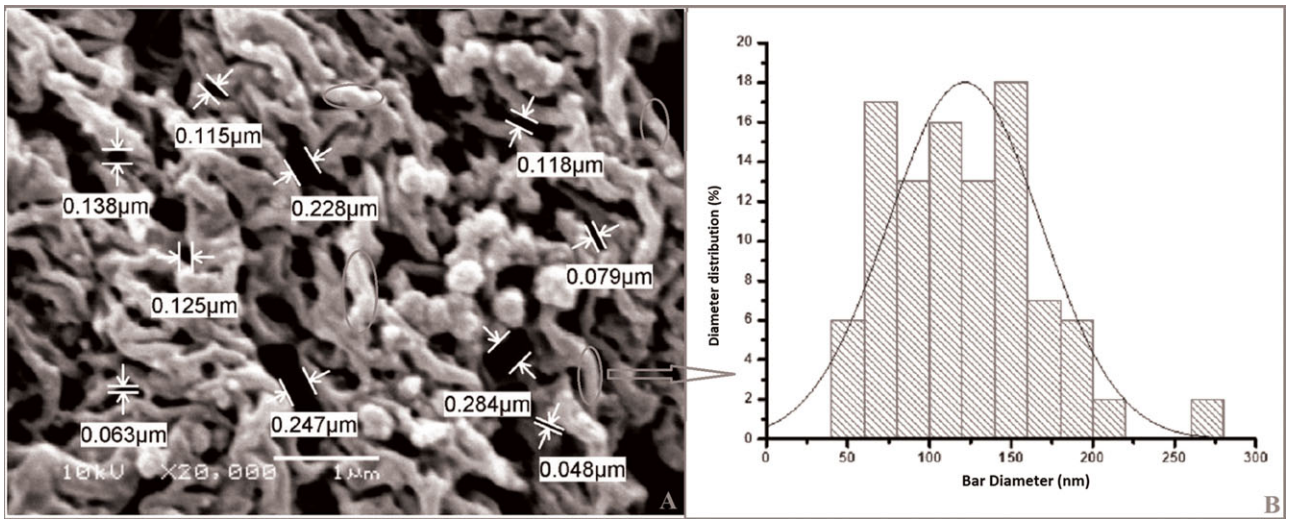

FIGURE 6. SEM images and bar diameter size distribution graph of porous alginate/AgNPs microbeads: (A) SEM images of porous alginate/AgNPs microbeads with the measurement of pore size and (B) bar diameter size distribution of porous alginate/AgNPs microbeads.

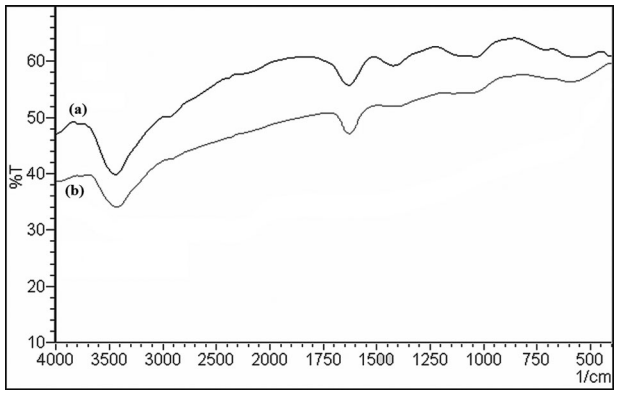

FIGURE 7. FTIR spectra of (a) alginate and (b) porous alginate/AgNPs microbeads.

ANTIBACTERIAL ACTIVITY

AgNPs containing biopolymers materials have strong bactericidal effects: inhibitory and cytotoxicity toward a broad spectrum of microorganisms as well as a broad range of antimicrobial activities. In this study, the antibacterial performance of alginate, alginate/AgNPs, and porous alginate/AgNPs microbeads was assessed against two Gram-positive strains, namely *S. aureus* (ATCC 25923) and *M. luteus* (ATCC 15307), and two Gram-negative strains, namely *E. coli* (ATCC 25922), and *P. aeruginosa* (ATCC 27853). Figure 8A shows the antibacterial effects of alginate, alginate/AgNPs microbeads, and nanoporous alginate/AgNPs microbeads using different concentrations of $AgNO_3$ (0.1–0.5 mol/L). Regarding the assay of the diameters by the zone of inhibition, the alginate/AgNPs microbeads and porous alginate/AgNPs microbeads showed an obvious good inhibition zone against all bacterial colonies, whereas alginate without AgNPs exhibited no inhibition zone, indicating nonantibacterial activity. This proves that the bactericidal activity of microbeads was due to AgNPs onto alginate and but not due to alginate itself. Moreover, the porous alginate/AgNPs microbeads showing higher antibacterial activity against Gram positive strains and Gram-negative strains than alginate/AgNPs microbeads. In addition, it was found that the antibacterial activity of the porous alginate/AgNPs increased with increasing the amount of AgNPs content, and the zone of inhibition also increased significantly. Figure 8B shows the antibacterial effects of alginate, alginate/AgNPs microbeads, and porous alginate/AgNPs microbeads synthesized with different concentrations of alginate (1-2%). The results showed that the alginate microbeads did not inhibit the growth of the four pathogenic bacteria, alginate/AgNPs microbeads and porous alginate/AgNPs showed antibacterial effect against all pathogenic organisms studied, and the porous alginate/AgNPs microbeads had higher antibacterial activity against all pathogenic organisms than those obtained for alginate/AgNPs microbeads. Results illustrated that Gram-positive bacteria were the most sensitive against alginate/AgNPs microbeads and porous alginate/AgNPs microbeads, and the Gram-negative bacteria were the least effective against all tested antimicrobial agents, and the porous alginate/AgNPs microbeads had higher antibacterial activity against all pathogenic organisms studied. The possible reasons were mainly attributed to the porous alginate/AgNPs microbeads pore structure and surface area.

The porous structure of alginate/AgNPs microbeads with greater pore size distribution and surface area leads to an increase in the content of AgNPs onto the surface of microbeads and release of AgNPs into the outer environment, thus displaying stronger antimicrobial activity toward pathogenic organisms than nonporous alginate/AgNPs microbeads.[33] Besides, it was also found that the appearance of the zone inhibitory and inhibition rate of the microbeads increased with increasing the AgNPs concentrations due to the higher AgNPs content onto the surface of porous microbeads, and the released amount of Ag in solution increased with time from the porous microbeads and its interaction with bacterial colonies and inactivates them, thus understanding a stronger antibacterial effectiveness of porous structure. So, the alginate/AgNPs with the porous structure are effective antibacterial agents against bacterial colonies and the

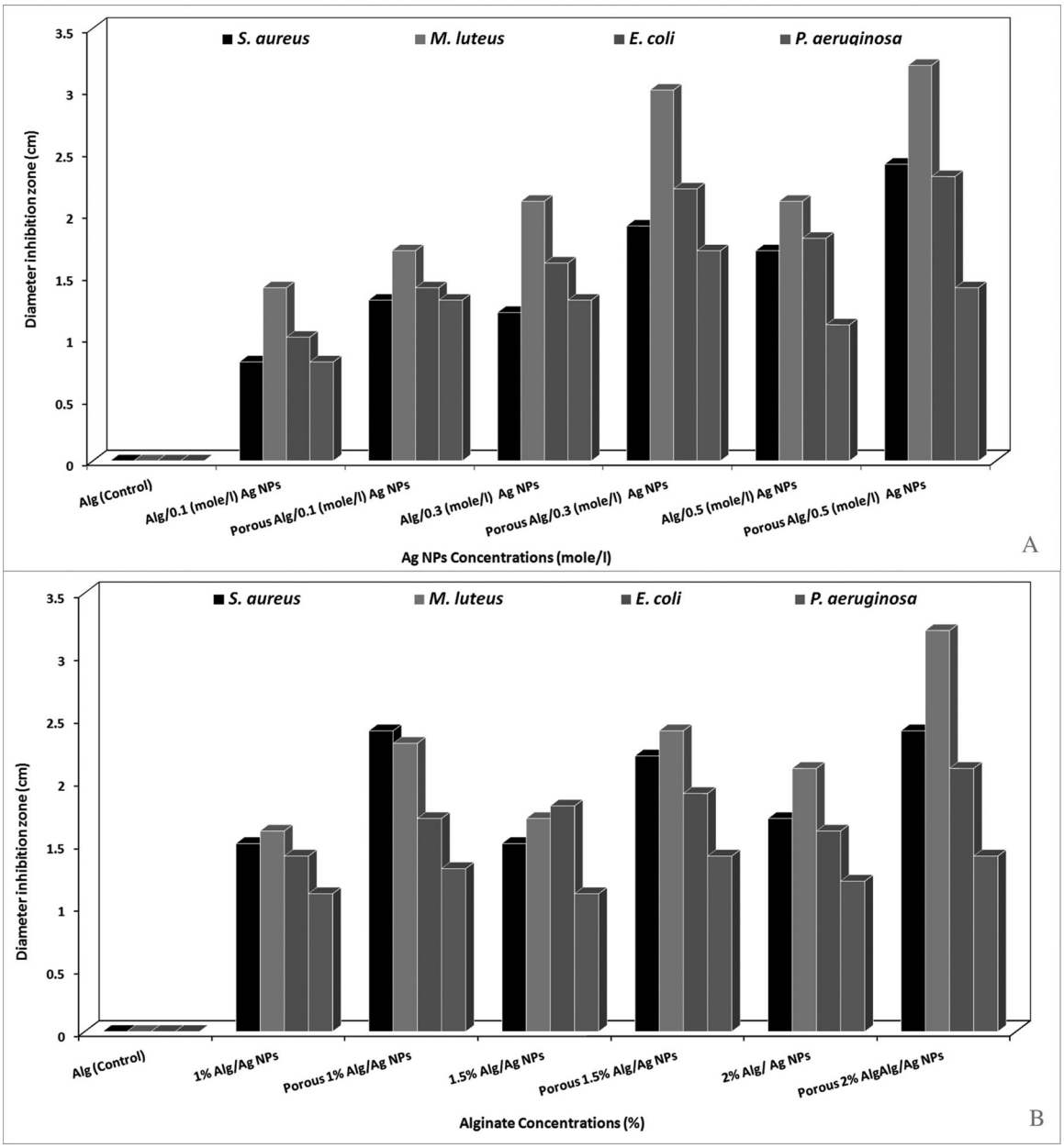

FIGURE 8. Antibacterial activities of (A) different concentrations of $AgNO_3$ (0.1–0.5 mol/L) and (B) different concentrations of alginate (1–2%); alginate, alginate/AgNPs microbeads, and porous alginate/AgNPs microbeads against *S. aureus*, *M. luteus*, *E. coli*, *P. aeruginosa*, respectively.

porous structure has a positive effect on the performance of antibacterial properties.

Conclusion

Spherical AgNPs were prepared in aqueous alkali hydrolyzed sodium alginate solution and then the microbeads containing AgNPs were prepared; alkali sodium alginate solution played the significant role in both as a reducing agent and stabilizing agent for the formed AgNPs and prevented the aggregation of nanoparticles. The porous structures of alginate/AgNPs microbeads were successfully prepared by using DMF containing AgNPs. The synthesis of AgNPs in alginate colloidal solutions and DMF solution was monitored by using TEM and UV–vis spectroscopy (AgNPs with an average size of 6–21 nm) with the narrowest size distribution. The alginate/AgNPs microbeads with the porous structure exhibit excellent antimicrobial activity against bacterial colonies and display higher antibacterial activity than alginate/AgNPs microbeads with the nonporous structure, and we conclude that the porous structure of microbeads greatly improves both antibacterial performance and release of silver ions into the outer environment of the material over nonporous microbeads.

Acknowledgments

This research was supported by Postdoc Foundation of Ministry of Education of China (Grant No is 2015M571457), National Nature Science Foundation of China (31470941, 31271035), Science and Technology Commission of Shanghai Municipality (15JC1490100, 15441905100), Ph.D. Programs Foundation of Ministry of Education of China (20130075110005) and light of textile project (J201404).

References

1. Liu, Y.; Chen, S.; Zhong, L.; Wu, G. J. Radiat Phys Chem 2009, 78, 251–255.
2. El-Aassar, M. R.; Hafez, E. E.; El-Deeb, N. M.; Fouda, M. M. G. Int J Biol Macromol 2014, 69, 88–94.
3. LeRoux, M.; Guilak, F.; Setton, L. J. Biomed Mater Res 1999, 47, 46–53.
4. Chai, Y.; Mei, L.; Lin, D.; Yao, S. J. Chem Eng Data 2004, 49, 475–478.
5. Mohy Eldin, M. S.; Seuror, E. I.; Nasr, M. A.; El-Aassar, M. R.; Tieama, H. A. J. Appl Biochem Biotechnol 2011, 164, 10–22.
6. Wang, X.; Wenk, E.; Hu, X.; Castro, G. R.; Meine, L. l.; Wang, X.; Li, C.; Merkle, H.; Kaplan, D. L. J. Biomaterials 2007, 28, 4161–4169.
7. Mohy Eldin, M. S.; Hassan, E. L.; El-Aassar, M. R. J. Dtsch Lebensm-Rundsch 2005, 101, 255–259.
8. Sugiura, S.; Oda, T.; Izumida, Y.; Aoyagi, Y.; Satake, M.; Ochiai, A.; Ohkohchi, N.; Nakajima M. J. Biomaterials 2005, 26, 3327–3331.
9. Lee, K. Y.; Peters, M. C.; Anderson, K. W.; Mooney, D. J. Nature 2000, 408, 998–1000.
10. Ho, M. H.; Kuo, P. Y.; Hsieh, H. J.; Hsien, T. Y.; Hou, L. T.; Lai, J. Y.; Wang, D. M. J. Biomaterials 2004, 25, 129–138.
11. Akamatsu, K.; Maruyama, K.; Chen, W.; Nakao, A.; Nakao, S. J. Colloid Interf Sci 2011, 363, 707–710.
12. Shiga, K.; Muramatsu, N.; Kondo, T. J. Pharm Pharmacol 1996, 48, 891–895.
13. Hu, W.; Peng, C.; Luo, W.; Lv, M.; Li, X.; Li, D.; Huang, Q.; Fan, C. J. ACS Nano 2010, 4, 4317–4323.
14. Pant, B.; Pant, H. R.; Pandeya, D. R.; Panthi, G.; Nam, K. T.; Hong, S. T.; Kim, C. S.; Kim, H. Y. J. Colloid Interf Sci 2012, 395, 94–99.
15. Pant, B.; Pant, R.; Barakat, N.; Park, M.; Jeon, K.; Choi, Y.; Kim, H. Y. J. Ceram Int 2013, 39, 7029–7035.
16. Fouda, M. M. G.; El-Aassar, M. R.; Al-Deyab, S. S. J. Carbohydr Polym 2013, 92, 1012–1017.
17. Abdel-Mohsen, A. M.; Aly, A. S.; Hrdina, R. J. Polym Environ 2012, 20, 459–468.
18. Abdel-Mohsen, M.; Rasha, M. A.; Fouda, M. M. G.; Vojtova, L.; Uhrova, A. F. J. Carbohydr Polym 2014, 102, 238–245.
19. Huang, L.; Liao, W.; Ling, H.; Wen, T. J. Mater Chem Phys 2009, 116, 474–478.
20. Saha, S.; Pal, A.; Pande, S.; Sarkar, S.; Panigrahi, S.; Pal, T. J. Phys Chem C 2009, 113, 7553–7560.
21. Rastogi, L.; Arunachalam, J. J. Mater Chem Phys 2011, 129, 558–563.
22. Saha, S.; Pal, A.; Kundu, S.; Basu, S.; Pal, T. J. Langmuir 2010, 26, 2885–2893.
23. Yoksan, R.; Chirachanchai, S. J. Mater Chem Phys 2009, 115, 296–302.
24. Rai, M.; Yadav, A.; Gade, A. J. Biotechnol Adv 2009, 27, 76–83.
25. Cai, J.; Kimura, S.; Wada, M.; Kuga, S. J. Biomacromolecules 2009, 10, 87–94.
26. Lee, S. W.; Mao, C.; Flynn, C. E.; Belcher, A. M. Science 2002, 296, 892–895.
27. Bhattacharjee, R.; Mandal, T. K. J. Colloid Interf Sci 2007, 307, 288–295.
28. Cui, Y. M.; Liu, L.; Li, B.; Zhou, X. F.; Xu, N. P. J. Phys Chem C 2010, 114, 2434–2439.
29. Wu, M.; Kuga, S.; Huang, Y. J. Langmuir 2008, 24, 10494–10497.
30. Zahran, M. K.; Ahmed, H. B.; El-Rafie, M. H. J. Carbohydr Polym 2014, 111, 10–17.
31. Pastoriza-Santos, I., Liz-Marzan, L. M. Tailoring the Morphology and Assembly of Silver Nanoparticles Formed in DMF, Nanoparticle Assemblies and Superstructures, CRC Press LLC: Boca Raton, FL, 2006; pp 525–550.
32. Khalil-Abad, M. S.; Yazdanshenas, M. E.; Nateghi, M. R. J. Cellulose 2009, 16, 1147–1157.
33. Guang, Y.; Jianjian, X.; Feng, H.; Zhangjun, C.; Xuexia, Y. J. Carbohydr Polym 2012, 87, 839–845.
34. Prasad, V.; D'Souza, C.; Yadav, D.; Shaikh, A. J.; Vigneshwaran, N.. Spectroscopic characterization of zinc oxide nanorods synthesized by solid-state reaction. Spectrochimica Acta A 2006, 65, 173–178.